Journal of Hazardous Materials 161 (2009) 1281–1287

Contents lists available at ScienceDirect

Journal of Hazardous Materials

journal homepage: www.elsevier.com/locate/jhazmat

Rapid photocatalytic destruction of pentachlorophenol in F–Si-comodified TiO_2 suspensions under microwave irradiation

Shaogui Yang[a,*], Hongbo Fu[b], Cheng Sun[a,*], Zhanqi Gao[a]

[a] State Key Laboratory of Pollution Control and Resource Reuse, School of the Environment, Nanjing University, Nanjing 210093, PR China
[b] Department of Environmental Science and Engineering, Fudan University, Shanghai 200433, PR China

ARTICLE INFO

Article history:
Received 18 March 2008
Received in revised form 19 April 2008
Accepted 21 April 2008
Available online 3 May 2008

Keywords:
F–Si-comodified TiO_2 (FST)
Photocatalytic degradation
Microwave irradiation
PCP

ABSTRACT

A novel photocatalysis material, F–Si-comodified TiO_2 (FST) powder, was synthesized by ultrasound-assisted hydrolysis. The prepared material was characterized by X-ray diffraction (XRD), X-ray photoelectron spectroscopy (XPS) and UV–visible absorption spectroscopy, respectively. XRD analysis indicated that the phase of FST was pure anatase and Si atoms suppressed the growth of titania crystalline, XPS spectra showed that FST was composed of Ti, O, Si and F element, the band gap energy of FST calculated according to the spectrum of UV–vis absorption was 3.26 eV. The electron spin resonance (ESR) spin-trapping technique using 5,5-dimethyl-1-pyrroline-*N*-oxide (DMPO) as the spin-trap reagent has been applied to detect free radical intermediates generated from FST. ESR results showed the concentration of the active species (•OH) on FST is higher than those on F-doping TiO_2 (FT), Si-modifying TiO_2 (ST) and P25 titania. The degradation of pentachlorophenol (PCP) in the microwave-assisted photocatalysis (MAPC) process was faster than other processes including microwave-assisted direct photolysis (MADP), microwave process alone (MP) and dark process (DP). The photocatalytic activity of FST is much higher than that of ST, FT and P25 titania. It may be attributed to its strong capacity of absorption to the UV–vis irradiation and more hydroxyl radical on surface of FST. In MPAC process, 40 mg L^{-1} PCP was completely degraded in 20 min and its corresponding mineralization efficiency was 71%, the pH of solutions decreased from 10.3 to 6.47 and the dechlorination was completed in 12 min. The intermediates products of PCP in MAPC process identified by GC/MS were trichlorophenols (TCP), tetrachlorophenols (TTCP) and tetrachlorocatechol (TTCC) and the possible mechanism of PCP degradation is proposed.

1. Introduction

Various approaches have been attempted to enhance the photocatalytic activity of TiO_2. Titania–silica mixed oxide [1,2] has aroused considerable interest for photocatalytic applications because of their high photocatalytic activity. This is partially explained in terms of the intimate interaction of TiO_2 and SiO_2 which results in new structural and physicochemical properties such as quantum-sized crystalline, high surface area, high adsorbability of reactant or high acidity [1,3,4].

Fluorinated TiO_2 has been often investigated in relation to doping ($TiO_{2-x}F_x$) [5–10] or surface complexation (F–TiO_2) [9–13]. It was reported that fluoride doping improves the crystallinity of anatase and the photocatalytic reactivity [6–8]. In addition, $TiO_{2-x}F_x$ has fewer anion vacancies with a lower density of midgap states [5–7,10] and is more stable against photocorrosion. Surface fluorinated TiO_2 (F–TiO_2) has been investigated as a new surface modification method [12,14,15]. Some researchers have reported that the introduction of fluorine atoms into a photocatalytic system is effective for enhancing the photocatalytic activity of TiO_2. The higher photocatalytic oxidation rate in the F–TiO_2 suspension has been ascribed to the enhanced generation of mobile free •OH radicals whereas most •OH radicals generated on naked TiO_2 surface prefer to remain adsorbed [14]. In our study, silicon and fluorine atoms were simultaneously comodified into the TiO_2 crystal lattice by ultrasound-assisted hydrolysis (UAH) with the aim of introducing new active sites while the UV–visible light absorption is improved. As a result, a highly reactive, photocatalyst (FST) would be achieved. However, to the best of our knowledge, the FST powder is firstly prepared.

Recent studies indicate that microwave-assisted photocatalysis (MAPC) is able to effectively destroy environmentally persistent pollutants and microwave irradiation could significantly improve the photocatalytic efficiency of TiO_2 for removal of pollutants [16–18]. In the paper, we report the preparation and photocatalytic

* Corresponding authors. Tel.: +86 25 83593239; fax: +86 25 83593239.
E-mail addresses: yangdlut@126.com, qhhh@nju.edu.cn (S. Yang), envidean@nju.edu.cn (C. Sun).

0304-3894/$ – see front matter © 2008 Elsevier B.V. All rights reserved.
doi:10.1016/j.jhazmat.2008.04.107

activity of F–Si-comodified TiO_2 by electron spin resonance (ESR) spin-trapping technique with a DMPO spin-trap reagent, investigate the rapid microwave-assisted photocatalytic degradation of PCP, which is one of the persistent toxic substance (PTS) and is carcinogenic and toxic to plants, animals, and human even at low concentrations.

2. Experimental

2.1. Materials

5,5-Dimethyl-1-pyrroline-*N*-oxide (DMPO) spin-trap reagent was brought from Sigma Chemical Co. All chemicals were reagent grade and used without further purification. Deionized and doubly distilled water were used throughout this study.

2.2. Preparation of FST powders

Tetrabutylorthotitanate (TBOT), tetraethylorthosilicate (TEOS) and NH_4F were used as titanium, silica and fluorine source, respectively. The mixture of TBOT (0.1125 mol) and TEOS was added dropwise to distilled water (900 mL) containing NH_4F under vigorous stirring at room temperature. When the atomic ratio of silicon to titanium was 10%, the atomic ratios of fluorine to titanium were 0%, 1%, the sample powders were labeled as ST and FST; when the atomic ratio of fluorine to titanium was 1%, the atomic ratio of silica to titanium was 0%, and the sample was labeled as FT. The samples were then irradiated with an ultrasonic cleaning bath (KQ3200E, 40 kHz, 150 W) for 1 h, followed by aging in a closed beaker at room temperature for 24 h. After aging, these samples were dried at 100 °C for about 8 h in air in order to vaporize water in the gels and then ground to fine powders to obtain dry gel samples. The dried gel samples were calcined at 550 °C in air for 1 h.

2.3. Characterization

The crystal phase of the sample was identified by X-ray diffraction with a X'TRA diffractometer (ARL company in Swiss). The optical absorption spectra of photocatalysts were recorded with a UV–vis spectrophotometer equipped with a diffuse reflectance attachment (Shimadzu UV-2401). X-ray photoelectron spectroscopy (XPS) measurements were done with an ESC ALB MK-II XPS System with a monochromatic Al KR source and a charge neutralizer. ESR signals of radicals spin-trapped by DMPO were recorded at ambient temperature on a Brucker ED-200D-SRC 10/12 spectrometer: the irradiation source was a UV–visible irradiation system (the maximum of wavelength = 365 nm, light power: 180 W). Hitachi Company Measurement of BET surface area was performed using N_2 adsorption/desorption isotherms on a Micromeritics ASAP 2020. The settings for the ESR spectrometer were as follows: center field, 3486.70 G; sweep width, 100 G; microwave frequency, 9.82 GHz; modulation frequency, 100 kHz; power, 5.05 mW.

2.4. Experimental procedure and analytical methods

All the experiments were carried out using a batch MW photoreactor, which was referred in our previous study [19]. EDLs (made by Nanjing Co. in China, 10 mm × 90 mm) were made of quartz and contained mercury and Ar introduced as a purge gas after bringing the system to 2.7 kPa. EDLs irradiated MW mainly emits bands at 254, 297, 313, 365, 405, 436, 546 577,579 nm, as presented in Fig. 1.

The initial concentration of PCP was 40 mg L^{-1} and photocatalysts were kept 0.18 g in all cases. Two electrodeless discharge lamps (EDLs) were used and the initial pH of solution was 10.3 in all cases.

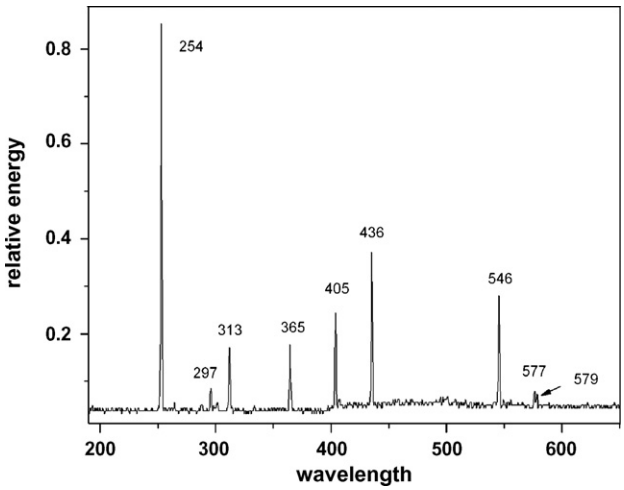

Fig. 1. The emission spectrum of EDML.

The samples at predetermined time were filtered with 0.20 μm Millipore to remove some particles that might clog the column. The filtrate was then analyzed as required. The determination of PCP concentrations was performed by HPLC (PU-1580, UV-1575, Jasco Corporation, Japan) with a Kromasil ODS (5 μm, 4.6 mm × 250 mm) reverse phase column. The mobile phase was 1.0 mL min^{-1} of methanol and water (V:V = 4:1) and the result was determined at 220 nm. The pH of solution was measured with pH meter (PHS-2C, China). And the variation of chloride ion evolution was measured by Chloride Ion-Selective Electrode (pCl-1, China). Total organic carbon (TOC) was determined with Shimadzu TOC-5000 analyzer. The reaction solutions were extracted with 25 mL dichloromethane plus 0.2 mL 30% HC1 and the procedure was repeated 3 times. The solvent fractions were combined and concentrated to 1 mL. Identification of intermediates was carried out with a GCQ coupled with a capillary column (DB-5MS, 30 m). The temperature ramp was as follows: 60 °C for 2 min, 65–120 °C at 35 °C min^{-1}, 120–300 °C at 7 °C min^{-1}, and at 300 °C hold for 5 min.

3. Results and discussion

3.1. Characterization of FST powders

XRD was used to investigate phase structure of FST, ST and FT after heat treatment at 550 °C for 1 h. Result was shown in Fig. 2. The major crystalline phase of all samples was pure anatase. It is apparently noted that apart from the diffraction peaks corresponding to anatase, no other diffraction peaks could be observed from 2θ = 20–60° for all samples. It can be seen from the figure that the peak intensity of FT is much higher than that of ST and FST, indicating that fluorine improves the crystallinity, which is in agreement with the report that fluorine doping improves the crystallinity of anatase and photocatalytic activity [6–8]. Moreover, the peaks of ST and FST are much wider than that of FT, which shows the average sizes of ST and FST are smaller than that of FT. Therefore, it is concluded that Si atom can suppress the growth of titania crystalline. The crystallite sizes of samples were calculated using the Debye–Scherrer equation [20] and the values for FT, ST and FST were 27, 4.9 and 7.1 nm, respectively.

The chemical forms and concentrations of the Si/F atoms in the FT, ST and FST powders were investigated. Fig. 3 shows the XPS spectra of FT, ST and FST powder calcined at 550 °C for 1 h. XPS peaks show that the FT powders contain only Ti, O, F element and a trace amount of carbon, the composition of ST powders is Ti, O, Si

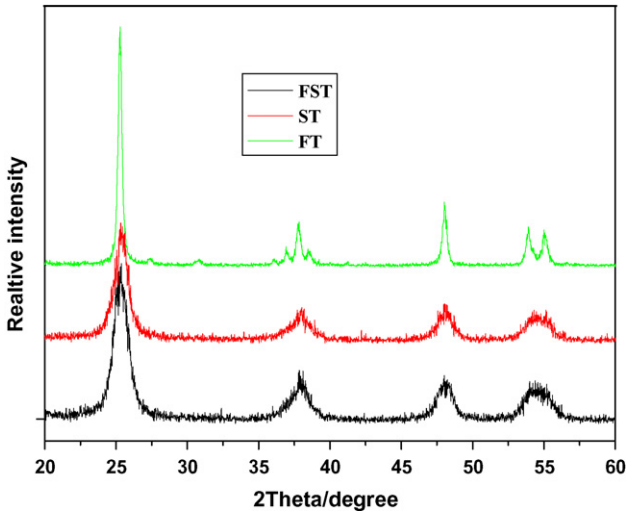

Fig. 2. XRD patterns of FST, FST and FT calcined at 550 °C for 1 h.

and carbon and the FST powders contain Ti, O, Si, F element and a trace amount of carbon. The following binding energies are used in our quantitative measurements: Ti 2p at 461 eV, O 1s at 533 eV, Si 2p at 103 eV, F 1s at 688 eV and C 1s at 287 eV. The atomic ratio of Ti:O:Si:F in FST sample is about 1:2.13:0.13:0.011, which is higher than the normal atomic composition of TiO_2, indicating that silicon atoms are partially concentrated on the surface region of the titania particles [21]. The C element in FT, ST and FST samples is ascribed to the residual carbon from precursor solution and the adventitious hydrocarbon from the XPS instrument itself.

It is important to study the optical absorption of the as-prepared nanoparticles because the UV–vis absorption edge is relevant to the energy band of semiconductor catalyst. Fig. 4 shows the UV–vis diffuse reflectance spectra (UV/Vis DRS) of FT, ST and FST. It can be seen from the figure that ST and FST show a blue shift in the band gap absorption edge was observed, which may be explained in terms of the quantum size effects that emerge in semiconductors at small particle sizes, and FT shows stronger absorption in the UV–visible range compared to ST and FST. The band gap energies of FT, ST and FST were calculated according to the Kubelka–Munk (K–M) theory [22]. The band gap energies of FT, ST and FST are about 3.20, 3.31 and 3.26 eV, respectively.

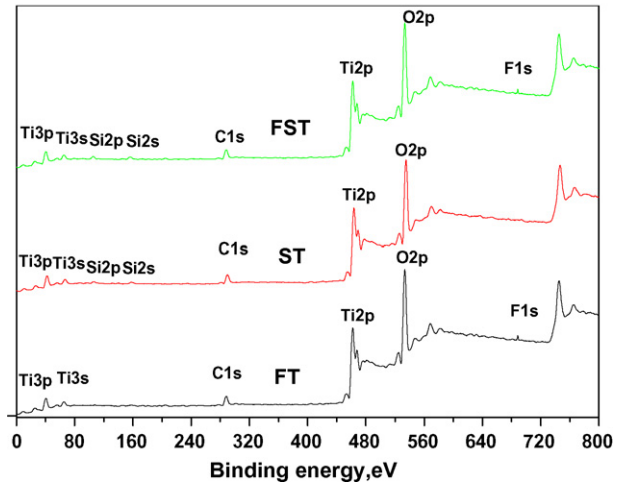

Fig. 3. XPS spectra of FT, ST and FST powders calcined at 550 °C for 1 h.

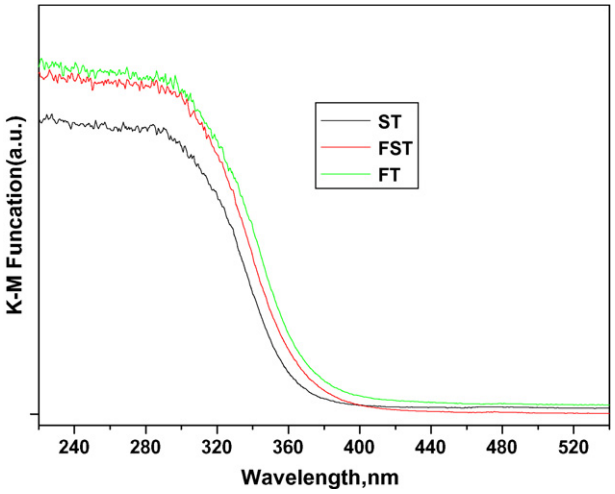

Fig. 4. UV–vis diffuse reflectance spectra of FST, ST and FT calcined at 550 °C for 1 h.

The surface area of the photocatalysts plays an important role in the photocatalytic process. It is noticed to enlarge the specific surface area of semiconductor to improve efficiency of photocatalysis. The specific surface areas of FT, ST and FST calcined at 550 °C for 1 h are 68, 196 and 163 $m^2\ g^{-1}$, which indicates that the mean size of ST is larger than those of FT and FST. It is documented that the smaller size of photocatalyst results in reducing the recombination rate of photogenerated holes and electrons to improve its photocatalytic activity [22].

3.2. ESR signal analysis of DMPO–OH

DMPO is a nitrone spin trap and it traps hydroxyl and superoxide radicals with the formation of nitrone spin adducts which are more stable and can be detected by ESR spectroscopy [23]. We employed the ESR spin-trap technique (with DMPO) to probe the nature of the reactive oxygen species generated during the irradiation of the present system. The experiments were carried out under UV irradiation, and the ESR signals at different irradiation time are shown in Fig. 5. No ESR signals were observed when the reaction was performed in the dark in the presence of FST or when DMPO alone was present. Under UV irradiation

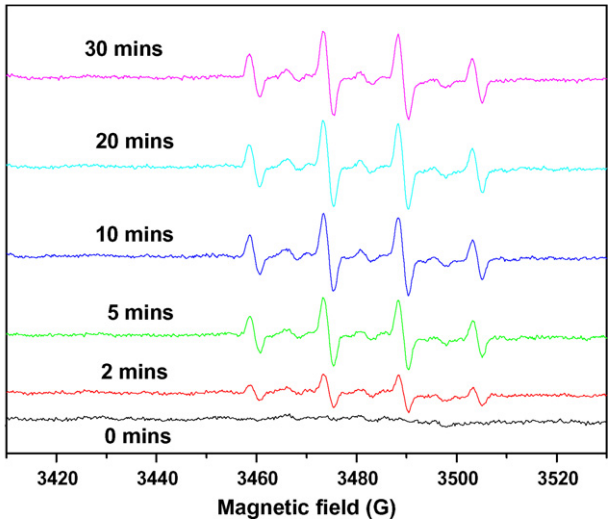

Fig. 5. DMPO spin-trapping ESR spectra of FST aqueous solutions after UV irradiation time. Catalyst loading, 0.5 g L^{-1}; DMPO concentration, 0.035 M.

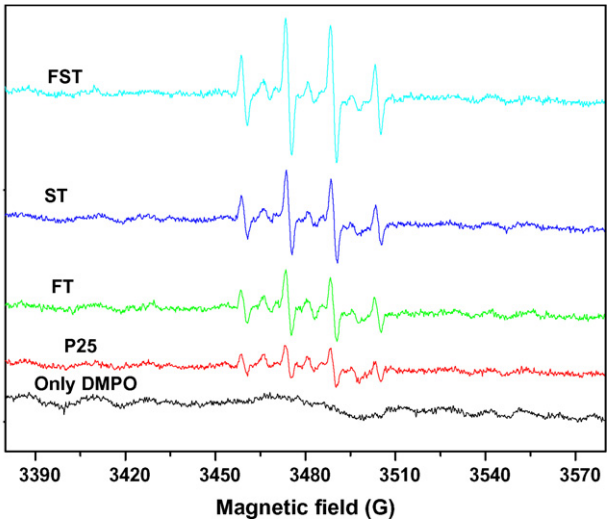

Fig. 6. DMPO spin-trapping ESR spectra of FST, ST, FT and P25 in aqueous solutions under UV irradiation for 10 min. Catalyst loading, 0.5 g L^{-1}; DMPO concentration, 0.035 M.

the characteristic quartet peaks of the DMPO–OH adduct with a 1:2:2:1 intensity observed, consist with the similar reports for the •OH adduct [24]. The parameters observed here for DMPO–OH are as follows, g is 2.00556, and $a_N = a_H$ is 14.95 G. The intensity of the peaks further increased with the increase of irradiation time and basically reached stable state in 10 min, therefore the intensity of the DMPO–OH adduct peak produced in 30 min irradiation was nearly similar to those in 10 and 20 min irradiation.

Fig. 6 illustrates the electron paramagnetic resonance spectra in different systems. It can be seen from the figure that there was no obvious ESR signals in the DMPO alone system, while in FST-DMPO, ST-DMPO, FT-DMPO and P25-DMPO system, the characteristic four peaks of DMPO–OH adduct with intensity 1:2:2:1,which is similar to spectra reported by others for the •OH adduct [25,26]. It confirms the formation of •OH radicals during the photocatalytic degradation of PCP in aqueous solution. It can be clearly observed from Fig. 5 that under the same experiment conditions the order of the peaks intensity of •OH generated from P25, ST, FT and FST was as follows: P25 < FT < ST < FST. The ESR signals for the spin adducts DMPO–OOH and/or DMPO–O_2^- should also have been detected. However, these latter two spin adducts were not observed under our experimental conditions. It is well documented that the superoxide radical anions are produced first and remain stable in an organic solvent medium [27,28]. When the fraction of H_2O is increased, such as occurs in a CH_3OH/H_2O mixed solvent system, the superoxide radical anion tends to be unstable, especially in H_2O alone. $O_2^{\bullet -}$ readily converted to H_2O_2 and O_2. The reactions between •OOH/O_2^- and DMPO are much slower than the formation of the DMPO–OH spin adduct [29,30]. And the transition from DMPO–OOH and DMPO–O_2^- to DMPO–OH was too fast [29,30].

3.3. *Microwave-assisted photocatalytic degradation of PCP*

The decay of PCP concentration of a function of reaction time is presented in Fig. 7. Degradation experiments of PCP in aqueous solution were carried out in four different processes: (a) dark process without microwave irradiation and photocatalyst (DP), (b) microwave process alone (MP), (c) microwave-assisted direct photolysis (MADP) by irradiation of electrodeless discharge lamps and (d) MAPC under irradiation of electrodeless discharge lamps. As shown in Fig. 7, the concentration of PCP is basically not changed

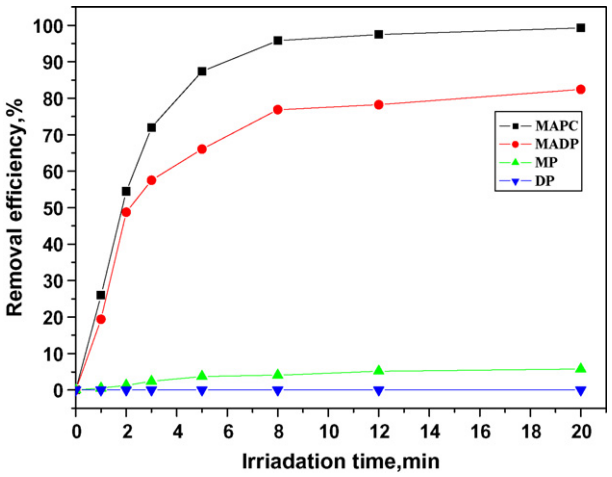

Fig. 7. Removal efficiency of 40 mg L^{-1} PCP in four different processes: (a) dark process (DP); (b) microwave process alone (MP); (c) MADP process; (d) MAPC process.

in the dark process during the whole period time. In MP, the degradation efficiency of PCP was only 5.9% in 20 min, which implied that PCP was not effectively degraded by microwave process alone and the heating effect of microwave resulted in the loss of PCP. It can be seen from the figure that in MADP, PCP was effectively decomposed and its removal was 82% in 20 min, because the ultraviolet (UV) radiation generated by the electrodeless discharge lamp can destroy PCP. While in MAPC (FST as photocatalyst), PCP was degraded quickly and its removal reached 99% in 20 min. It was noted that the difference in removal efficiency between MAPC and MADP was observed remarkably after 2 min irradiation time, probably because the photocatalytic effect was obvious after the long irradiation time.

To test the mineralization degree of PCP, TOC variation of PCP vs. irradiation time was plotted in Fig. 8. It is clearly observed that TOC values of PCP solutions in both DP and MP processes did not change basically, namely, mineralization did not occur in both processes as mentioned above. While mineralization efficiencies of PCP solutions in MADP and MAPC processes were 55% and 71%, respectively. It indicated that PCP in aqueous solutions was decomposed and mineralized rapidly in 20 min using MAPC technology. Yang et

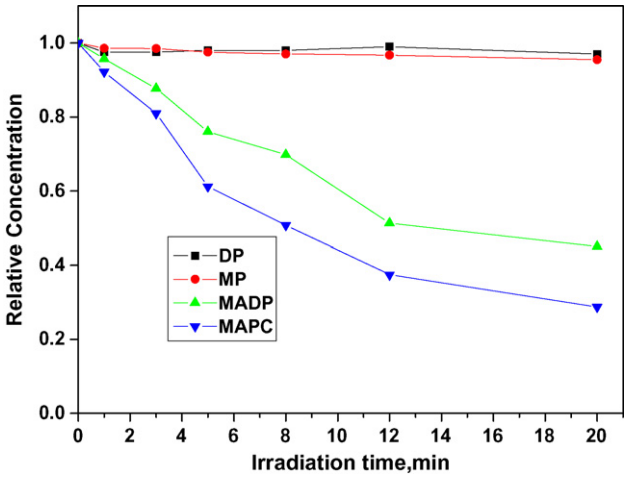

Fig. 8. The variation of TOC relative concentration vs. irradiation time in different treatment processes. DP is direct photolysis; MP is microwave process alone; MADP is microwave-assisted direct photolysis; MAPC is microwave-assisted photocatalysis.

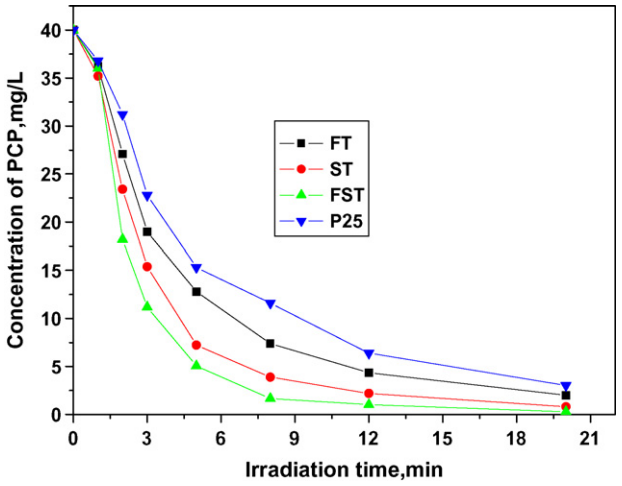

Fig. 9. Concentration variation of PCP vs. UV irradiation time in different photocatalysts under microwave irradiation.

al. [22] reported that about 49% of 40 mg/L PCP in aqueous solution was mineralized by photoelectrocatalytic degradation in 3 h. Therefore, the photocatalytic degradation efficiency of PCP in aqueous solutions can be effectively improved by microwave or electric field and so on.

The very rapid degradation of PCP in MAPC process is possibly attributed to the following reasons: firstly, intense UV light generated by the electrodeless discharge lamp in the microwave field result in the direct photolytic degradation of PCP. Secondly, active free radical (such as •OH and •OOH) on the surface of catalyst under UV irradiation can effectively decompose PCP. Thirdly, more •OH radicals on photocatalysts are generated in microwave field. Horikoshi et al. [16] proved that about 20% more •OH radicals were produced by MAPC process than photocatalysis alone. Finally, microwave also generated additional defect sites on the catalyst, which probably decreased the recombination of photogenerated holes and electrons [17,18]. In addition, the hydrophilicity of the photocatalyst surfaces under microwave radiation results in desorption of water molecules in the surface of catalyst, which likely inhibits the reactants from attaching to active sites of oxidation on the catalyst surface [29]. Therefore, PCP was very rapidly decomposed and even effectively mineralized in MAPC process.

3.4. Comparison of photocatalytic activity

The photocatalytic degradation of PCP over FST, ST, FT and P25 titania powders was carried out in same experiment condition. The result was presented in Fig. 9. It can be seen from the figure that FST, FT, ST and P25 exhibit different photocatalytic activity. In 12 min, about 97% of PCP was degraded by FST, while degradation efficiencies of PCP for ST, FT and P25 were 94.5%, 89% and 84%, respectively. For such photochemical reactions, a plot of initial degradation rate vs. the initial concentration of substrate is found to follow Langmuir–Hinshewood or Michaelis–Menden kinetics [30]. The determined reaction rate constants for FST, ST, FT and P25 titania are 0.2851, 0.2231, 0.1683 and 0.1399 min^{-1}, respectively. In other words, the photocatalytic activity of FST is the best among FST, ST, FT and P25 and its photocatalytic degradation rate was over 2 times of that on P25. This result implied that Si and F simultaneously doping for TiO_2 took an important role in the enhancement of photoactivity. The high photocatalytic activity of FST may be attributed to more hydroxyl radical (shown in Fig. 8), good anatase crystallinity presented in Fig. 2 and high UV absorption shown in Fig. 4. Therefore, Si and F simultaneously doping for TiO_2 is an effective and feasible approach for achieving highly effective photocatalysis.

3.5. The variation of pH and Cl ion

Generally speaking, in photocatalytic degradation of PCP, the attack of active radicals (such as •OH, •OOH) to PCP may replace chlorine atoms, producing more hydroxyl functional groups that can be oxidized to aldehyde and/or further oxidation to open up the aromatic ring [31,32]. The opening up of the aromatic ring may produce organic dicarboxylic acids, such as oxalic acid, before complete mineralization. It can be inferred that pH will decrease during the course of reaction while chloride ion will evolve. It is apparent that before complete mineralization occurs, some intermediate may be produced. Therefore, in order to gain a better comprehension of the process for photocatalytic degradation PCP, we conducted studies of the variation of pH and chloride ion in solutions vs. the irradiation time [32].

The pH variation of PCP solutions with different technology is shown in Fig. 10. In MADP process, the pH of solutions decreased from 10.3 to 7.4 in 20 min, while in MAPC process, it changed from 10.3 to 6.47 at the same time. It may be caused by the generation of H^+ produced by the reaction intermediates of PCP attacked further by •OH. The variation of Cl^- in the MPAC and MADP process was presented in Fig. 10. In MADP process, the decolorized process was basically completed in 20 min, as to MAPC process, it was completed in 12 min. It can be seen that the Cl^- amount increased obviously along with the degradation of PCP. It indicated that the chlorine atom was first removed, because the breaking of C–Cl bond is energetically more favorable than that of C–OH bond (the bond dissociated energy for a C–Cl bond is approximately 10 kcal/mol less than that for a C–OH bond) [33].

3.6. Mechanistic considerations in the photodegradation of PCP

The degradation products of PCP in MAPC process were identified by GC/MS. As shown in Fig. 11, the major intermediates were tetrachlorophenol (TTCP) and tetrachlorocatechol (TTCC) in 1.5 min, while in 3.5 min, the products were trichlorophenols (TCP), tetrachlorophenols (TTCP) and tetrachlorocatechol (TTCC). The PCP significantly absorbs UV wavelengths, so that in the present context, the degradation of PCP likely to proceed following two pathways: namely, photocatalytic degradation and direct photolysis.

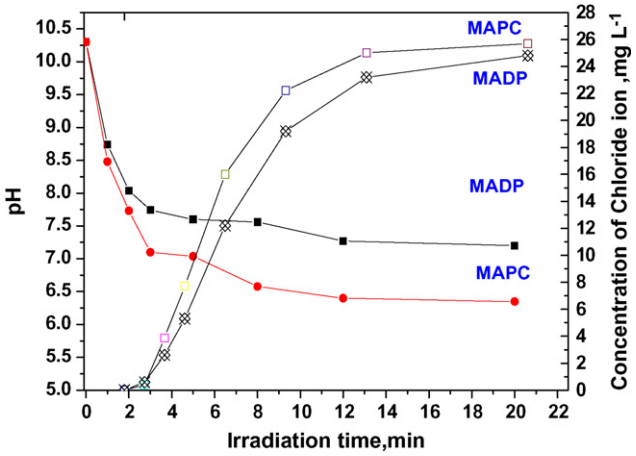

Fig. 10. pH change and chloride ion evolution in the MADP and MAPC processes.

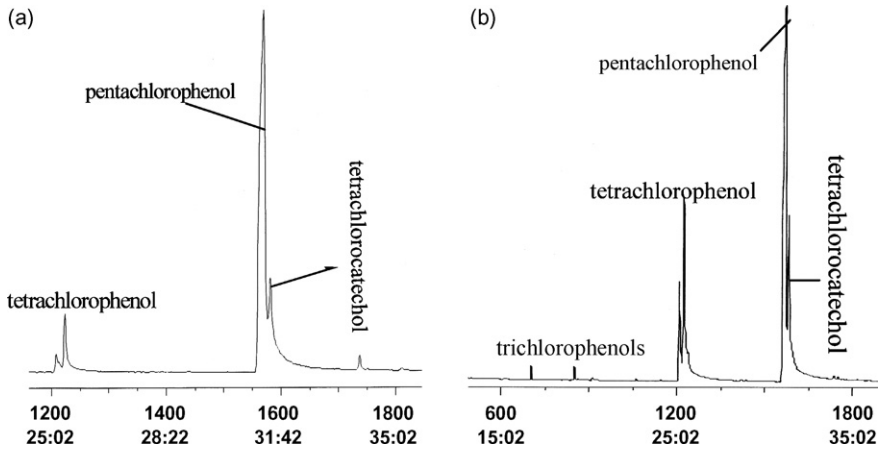

Fig. 11. GC/MS spectra of intermediate product of PCP in MPC degradation: (a) 1.5 min and (b) 3.5 min.

3.6.1. Photocatalytic degradation

Firstly, FST absorbs UV light at energies greater than the band gap energy of 3.29 eV to generate electron/hole pairs. After separation, the valence band holes (h^+_{VB}) migrate to and get trapped by the surface HO^- ions (or by H_2O) to yield •OH radicals. Concomitantly, surface adsorbed oxygen molecules scavenge the conduction band electrons (e-CB) to yield superoxide radical anions, $O_2^{\bullet -}$, which can combine with protons (H^+) to generate the •OOH radicals. Photooxidation of PCP takes place by •OH radical/h^+_{VB} attack on the positions of highest electron density in the PCP molecules and product TTCP, TTCC and TCP, as shown in Fig. 12. PCP is first oxidized into TTCP, and then further changed into TCPT, TCC and the opening of the ring, and finally the complete mineralization to H_2O and CO_2. Oxidation by HOO• radicals is expected to be relatively insignificant as the kinetics are several orders of magnitude slower than for the •OH radicals [21,22]. Note that the direct photodegradation of PCP by direct trapping of valence band holes poised on the FST surface is not precluded but is likely a minor step.

3.6.2. Direct photolysis

In this mechanism, the direct photolysis of PCP under UV irradiation can be separated into the following partial reactions:

Activation of a PCP molecule by the absorption of one photon, leading to an excited molecule (Eq. (1)), occurred firstly. Then PCP reductive dechlorination (Eq. (2)) was observed and formed some intermediates, finally mineralized (Eq. (3)), similarly to what occurs in the UV–irradiation of PCP in aqueous solutions [34]

$$PCP + h\nu \rightarrow PCP^* \quad (1)$$

$$PCP^* + h\nu \rightarrow \text{intermediates(TTCP, TCP, TCC)} + x\text{Cl}^- \quad (2)$$

$$\text{Intermediates} + h\nu \rightarrow CO_2 + H_2O \quad (3)$$

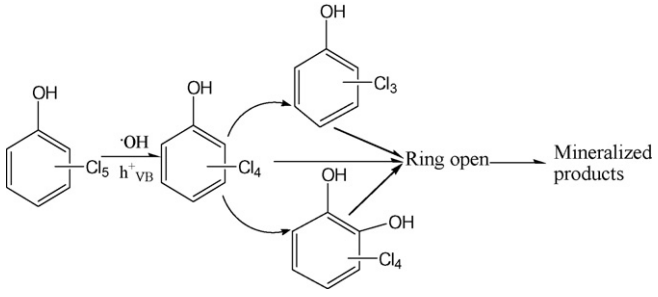

Fig. 12. Photocatalytic degradation mechanism of PCP under microwave irradiation.

In addition, free chloride ions are generated in these dechlorination steps.

4. Conclusions

Fi–Si-comodified titania (FST) was successfully prepared firstly and characterized. Results showed that the phase of FST was pure anatase and its band gap energy was about 3.26 eV. And it is inferred from ESR signal that hydroxyl radicals (•OH) generated from FST participate in the photocatalysis process, although they may not be the sole species. The degradation of PCP in microwave-assisted photocatalytic process is faster than that in microwave-assisted photolytic and microwave process alone and dark process (DP). It may be attributed to the intensive UV irradiation from EDLs radiated by microwave field, an excellent photocatalyst (FST) and microwave irradiation.

The photocatalytic activity of FST was much higher than those of FT, FST and P25 titania. This may be ascribed to its more hydroxyl radical, good anatase crystallinity, high UV absorption. PCP was effectively degraded in the MAPC process on FST. In MAPC process, the removal of 40 mg/L PCP in aqueous suspension was 100% in 20 min and its corresponding mineralization efficiency was 71%, and the pH of reaction solution decreased from 10.3 to 6.47 and the process of dechlorination was completed in 12 min. The intermediates products of PCP in MAPC process identified by GC/MS were trichlorophenols, tetrachlorophenols and tetrachlorocatechol.

Acknowledgments

This work was supported by National Nature Science Foundation of P.R. China (Project Nos. 20707009 and 20737001) and Jiangsu Province Social Development Foundation (BS2007051) for financial support.

References

[1] N. Husing, B. Launay, D. Doshi, G. Kickelbick, Mesostructured silica-titania mixed oxide thin films, Chem. Mater. 14 (2002) 2429–2432.
[2] V. Lafond, H. Mutin, A. Vioux, Control of the texture of titania-silica mixed oxides prepared by nonhydrolytic sol–gel, Chem. Mater. 16 (2004) 5380–5386.
[3] R. Mariscal, M. Lopez-Granados, J.L.G. Fierro, C. Martos, R. Van Grieken, Morphology and surface properties of titania-silica hydrophobic xerogels, Langmuir 16 (2000) 9460–9467.
[4] D.C.M. Dutoit, M. Schmeider, A. Baiker, Titania-silica mixed oxides: I. influence of sol–gel and drying conditions on structural properties, J. Catal. 153 (1995) 165–176.
[5] S.N. Subbarao, Y.H. Yun, R. Kershaw, K. Dwight, A. Wold, Electrical and optical properties of the system $TiO_{2-x}F_x$, Inorg. Chem. 18 (1979) 488–492.

[6] A. Hattori, M. Yamamoto, H. Tada, S. Ito, A promoting effect of NH_4F addition on the photocatalytic activity of sol–gel TiO_2 films, Chem. Lett. 8 (1998) 707–708.
[7] A. Hattori, K. Shimoda, H. Tada, S. Ito, Photoreactivity of sol–gel TiO_2 films formed on soda-lime glass substrates: effect of SiO_2 underlayer containing fluorine, Langmuir 15 (1999) 5422–5425.
[8] J.C. Yu, J.G. Yu, W.K. Ho, Z.T. Jiang, L.Z. Zhang, Effects of F-doping on the photocatalytic activity and microstructures of nanocrystalline TiO_2 powders, Chem. Mater. 14 (2002) 3808–3816.
[9] C.M. Wang, T.E. Mallouk, Photoelectrochemistry and interfacial energetics of titanium dioxide photoelectrodes in fluoride-containing solutions, J. Phys. Chem. 94 (1990) 423–428.
[10] C.M. Wang, T.E. Mallouk, Wide-range tuning of the titanium dioxide flat-band potential by adsorption of fluoride and hydrofluoric acid, J. Phys. Chem. 94 (1990) 4276–4280.
[11] C. Minero, G. Mariella, V. Maurino, D. Vione, E. Pelizzetti, Photocatalytic transformation of organic compounds in the presence of inorganic ions. 2. Competitive reactions of phenol and alcohols on a titanium dioxide-fluoride system, Langmuir 16 (2000) 8964–8972.
[12] M.S. Vohra, S. Kim, W. Choi, Effects of surface fluorination of TiO_2 on the photocatalytic degradation of tetramethylammonium, J. Photochem. Photobiol. A 160 (2003) 55–60.
[13] M. Lewandowski, D.F. Ollis, Halide acid pretreatments of photocatalysts for oxidation of aromatic air contaminants: rate enhancement, rate inhibition, and a thermodynamic rationale, J. Catal. 217 (2003) 38–46.
[14] C. Minero, G. Mariella, V. Maurino, E. Pelizzetti, Photocatalytic transformation of organic compounds in the presence of inorganic anions. 1. Hydroxyl-mediated and direct electron-transfer reactions of phenol on a titanium dioxide-fluoride system, Langmuir 16 (2000) 2632–2641.
[15] H. Park, W.J. Choi, Effects of TiO_2 surface fluorination on photocatalytic reactions and photoelectrochemical behaviors, J. Phys. Chem. B 108 (2004) 4086–4093.
[16] S. Horikoshi, H. Hidaka, N. Serpone, Environmental remediation by an integrated microwave/UV-illumination method. 1. Microwave-assisted degradation of Rhodamine-B dye in aqueous TiO_2 dispersion, Environ. Sci. Technol. 36 (2002) 1357–1366.
[17] Z.H. Ai, P. Yang, X.H. Lu, Degradation of 4-chlorophenol by a microwave assisted photocatalysis method, J. Hazard. Mater. 124 (2005) 147–152.
[18] D.Z. Li, Y. Zheng, Z.X. Fu, Study on the effect and mechanism of the coupling between microwave and photocatalysis, Acta Phys.-Chim. Sin. 23 (2002) 2351–2354.
[19] Y.Z. Liu, S.G. Yang, J. Hong, C. Sun, Low-temperature preparation and microwave assisted photocatalytic activity study of TiO_2-mounted activated carbon, J. Hazard. Mater. 142 (2007) 208–215.
[20] S.G. Yang, X. Quan, X.Y. Li, Preparation, characterization and photoelectrocatalytic properties of nanocrystalline Fe_2O_3/TiO_2, ZnO/TiO_2, and Fe_2O_3/ZnO/TiO_2 composite film electrodes towards pentachlorophenol degradation, Phys. Chem. Chem. Phys. 6 (2004) 654–659.
[21] D.W. Lee, S.K. Ihm, K.H. Lee, Mesostructure control using a titania-coated silica nanosphere framework with extremely high thermal stability, Chem. Mater. 17 (2005) 4461–4467.
[22] S.G. Yang, Y.Z. Liu, C. Sun, Preparation of anatase TiO_2/Ti nanotube-like electrodes and their high photoelectrocatalytic activity for the degradation of PCP in aqueous solution, Appl. Catal. A: Gen. 301 (2006) 284–2491.
[23] E. Finkelstein, G.M. Rosen, E.J. Rauckman, Spin trapping of superoxide and hydroxyl radical: practical aspects, Arch. Biochem. Biophys. 200 (1980) 1–16.
[24] Y. Huang, J. Li, W. Ma, M. Cheng, J. Zhao, Efficient H_2O_2 oxidation of organic pollutants catalyzed by supported iron sulfophenylporphyrin under visible light irradiation, J. Phys. Chem. B 108 (2004) 7263–7270.
[25] H. Hidaka, J. Zhao, E. Pelizzetti, N. Serpone, Photodegradation of surfactants. 8. Comparison of photocatalytic processes between anionic DBS and cationic BDDAC on the titania surface, J. Phys. Chem. 96 (1992) 2226–2230.
[26] J. Kochany, J.R. Bolton, Mechanism of photodegradation of aqueous organic pollutants. 1. EPR spin-trapping technique for the determination of hydroxyl radical rate constants in the photooxidation of chlorophenols following the photolysis of hydrogen peroxide, J. Phys. Chem. 95 (1991) 5116–5170.
[27] C. Chen, X. Li, W. Ma, J. Zhao, H. Hidaka, N. Serpone, Effect of transition metal ions on the TiO_2-assisted photodegradation of dyes under visible irradiation: a probe for the interfacial electron transfer process and reaction mechanism, J. Phys. Chem. B 106 (2002) 318–324.
[28] C. Chen, W. Zhao, P. Lei, J. Zhao, N. Serpone, Photosensitized degradation of dyes in polyoxometalate solutions versus TiO_2 dispersions under visible-light irradiation: mechanistic implications, Chem-Eur. J. 10 (2004) 1956–1965.
[29] S. Horikoshi, H. Hidaka, N. Serpone, Environmental remediation by an integrated microwave/UV-illumination method. II. Characteristics of a novel UV–vis-microwave integrated irradiation device in photodegradation processes, J. Photochem. Photobiol. A: Chem. 153 (2002) 185–189.
[30] J. Zhao, T. Wu, K. Wu, K. Oikawa, H. Hidaka, N. Serpone, Photoassisted degradation of dye pollutants. 3. Degradation of the cationic dye rhodamine B in aqueous anionic surfactant/TiO_2 dispersions under visible light irradiation: evidence for the need of substrate adsorption on TiO_2 particles, Environ. Sci. Technol. 32 (1998) 2394–2400.
[31] G. Mills, M.R. Hoffmann, Photocatalytic.degradation of pentachlorophenol on titanium dioxide particles: identification of intermediates and mechanism of reaction, Environ. Sci. Technol. 27 (1993) 1681–1689.
[32] S.G. Yang, X. Quan, X.Y. Li, C. Sun, Photoelectrocatalytic treatment of PCP in aqueous solution over rutile nanotube-like TiO_2/Ti electrode, Photochem. Photobiol. Sci. 5 (2006) 808–814.
[33] M.A. Boncz, H. Bruning, W.H. Bulkens, Kinetic mechanistic aspects of the oxidation of chlorophenols by ozone, Water Sci. Technol. 35 (1997) 65–72.
[34] L.P. Emmanuel, K.D. David, The photochemical mineralization of pentachlorophenol in a tropical marine environment, J. Photochem. Photobiol. A 135 (2000) 81–84.